The Oxide $Ba_6Ga_2Co_{11}O_{26}$: A New Close-Packed Stacking Derived from the Hexagonal Perovskite

D. Pelloquin,* O. Pérez, G. Martinet, S. Hébert, and A. Maignan

Laboratoire CRISMAT, UMR6508 CNRS-ENSICAEN, 6 boulevard Maréchal Juin, 14050 CAEN Cedex, France

Received January 30, 2007. Revised Manuscript Received March 13, 2007

Single crystals of a new compound, $Ba_6Ga_2Co_{11}O_{26}$, have been grown by a self-flux method. The structure determined by single-crystal X-ray diffraction and transmission electron microscopy (TEM) techniques shows a complex intergrowth between an hexagonal perovskite block, corresponding to the 5H term, and a complex block $[Ba(Ga,Co)_8O_{11}]$. It crystallizes in the $P\bar{3}m1$ trigonal space group with the following unit-cell parameters: $a = 5.652(2)$ Å, $b = 5.652(2)$ Å, $c = 18.828(8)$ Å, and $\gamma = 120°$. The structural analogy with two structural types, namely rocksalt and nolanite, allows a description of the nature of the $[Ba(Ga,Co)_8O_{11}]$ block: one central $[111]^{RS}$ Co_4O_8 slab, related to a CdI_2-type slice, is sandwiched between two $Ba(Ga,Co)_2O_3$ nolanite-type slabs containing $(Co/Ga)O_4$ tetrahedra and $(Co/Ga)O_6$ octahedra. This compound can be thus viewed as the $n = 5$ member of the large series $[Ba(Ga,Co)_8O_{11}][BaCoO_3]_n$, opening the route toward the discovery of new cobaltites.

Introduction

In the seventies, the possibility to use layered cobaltites A_xCoO_2 (A = alkaline cations) as cathode materials in batteries has shown the importance of such metal transition oxides for applications.[1] This has been also more recently illustrated by the promising thermoelectric oxides whose layer structures contain similar CdI_2-type slabs made of edge-sharing CoO_6 octahedra as $Na_{0.5}CoO_2$[2] and misfit cobaltites $[Ca_2CoO_3][CoO_2]_{1.62}$.[3] The structure of the latter can be described as the intergrowth between one cobalt CdI_2-type type and three rock salt-RS type layers, whereas the structure of the former corresponds to alternating CoO_2 and partially filled Na^+ layers.

In all these cobaltites, the CdI_2-type structure made of frustrated triangular cobalt network favors the stabilization of the Co^{3+} ($S = 0$)/Co^{4+} ($S = 1/2$) low-spin states responsible for the metallicity.[4] Such a combination of geometric frustrations and weak magnetic moments can explain the lack of magnetic ordering. This situation is in marked contrast with the strong antiferromagnetism reported in other layered cobaltites, for which the CoO_2 perovskite-type layer with corner-shared CoO_6 octahedra favors cobalt species with higher-spin states as illustrated in the brown-millerite $Sr_2(Co,Ga)_2O_5$[5] and in the 2201-like structure $(Ga_{1/3}Co_{2/3})_2Sr_2CoO_{6+d}$.[6] The recent reports of the $SrCo_6O_{11}$ oxide[7] and the $Ba_{n+1}Co_nO_{3n+3}(Co_8O_8)$ series ($n = 1, 2$)[8] have also opened interesting possibilities. For the latter, the structural studies from single crystals, prepared by a flux method, showed that they crystallize within a structure built from Co_4O_8 CdI_2-type layers, including four extra cobalts sitting at the interface with a block of hexagonal perovskite layers, one or two octahedra layers thick, leading to the members $Ba_2Co_9O_{14}$ ($n = 1$) and $Ba_3Co_{10}O_{17}$ ($n = 2$), respectively.[8] In the case of $SrCo_6O_{11}$,[7] prepared under high pressures, it was shown that the structure contains blocks of Co_3O_8 spinel-type layers and exhibits relationships with the $BaTi_2Fe_4O_{11}$[9] and the magnetoplumbite $BaGa_{12}O_{19}$ structures.[10] Thus, the discovery of new layered cobaltites, in which cobalt layers derived from CdI_2-type or spinel structures are intergrown with other structural types, is an exciting challenge for the solid-state chemist community with the aim of generating new physical properties.

This paper deals with the crystal growth and structural study of a new layered oxide, namely $Ba_6Ga_2Co_{11}O_{26}$. A structural mechanism is proposed to describe this compound. It results from a complex intergrowth between a hexagonal $BaCoO_3$ perovskite that is five octahedral layers thick sharing a common $[BaO_3]$ layer with an unusual $BaGa_2Co_6O_{11}$ layer block derived from the nolanite and RS-type structures. Structural relationships with the $n = 5$ member of the $Ba_{n+1}Co_nO_{3n+3}(Co_8O_8)$[8] series are also made, whereas the Ga^{3+}

* Corresponding author. E-mail: denis.pelloquin@ensicaen.fr.

(1) Fouassier, C.; Delmas, C.; Hagenmuller, P. *Mater. Res. Bull.* **1975**, *10*, 443.
(2) Terasaki, I.; Sasago, Y.; Uchinokura, K. *Phys. Rev. B* **1997**, *56*, R12685.
(3) Masset, A. C.; Michel, C.; Maignan, A.; Hervieu, M.; Toulemonde, O.; Studer, F.; Raveau, B.; Hejtmanek, J. *Phys. Rev. B* **2000**, *62*, 166.
(4) Koshibae, W.; Tsutsui, K.; Maekawa, S. *Phys. Rev. B* **2000**, *62*, 68−69.
(5) Lindberg, F.; Ya Istomin, S.; Berastegui, P.; Swensson, G.; Kazakov, S. M.; Antipov, E. V. *J. Solid State Chem.* **2003**, *173*, 395.
(6) Pelloquin, D.; Hébert, S.; Pérez, O.; Pralong, V.; Nguyen, N.; Maignan, A. *J. Solid State Chem.* **2005**, *178*, 792.
(7) Ishiwata, S.; Wang, D.; Saito, T.; Takano, M. *Chem. Mater.* **2005**, *17*, 2789.
(8) Sun, J.; Yang, M.; Li, G.; Yang, T.; Liao, F.; Wang, Y.; Xiong, M.; Lin, J. *Inorg. Chem.* **2006**, *45*, 9151.
(9) Haberey, F.; Velicescu, M. *Acta Crystallogr., Sect. B* **1974**, *30*, 1507.
(10) Bertaut, F.; Deschamps, A.; Pauthenet, R.; Pickart, S. *J. Phys. Radium* **1959**, *20*, 404.

10.1021/cm0702823 CCC: $37.00
Published on Web 04/18/2007

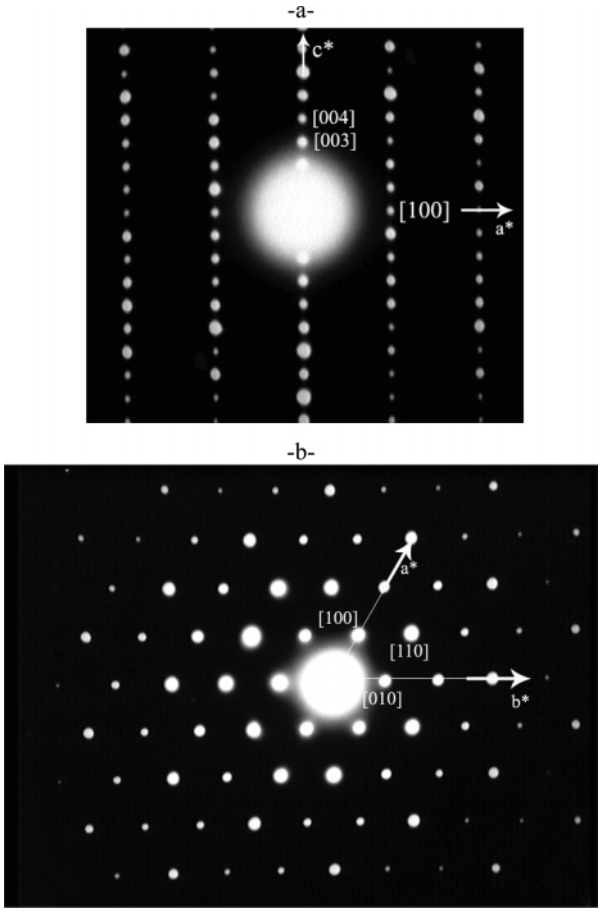

Figure 1. Experimental electron diffraction patterns oriented along (a) [010] and (b) [001] directions. Spots are indexed in the trigonal $P\bar{3}m1$ space group.

affinity with the tetrahedral coordination is thought to play a crucial role for the formation of this new structural series.

Experimental Section

First, a polycrystalline precursor has been prepared by a solid-state route from BaO_2, Ga_2O_3, and Co_3O_4 precursors according to the nominal 6:1:3 composition. The powder was intimately mixed and ground in mortar. Next, the mixture was pressed as bars and encapsulated in an alumina finger and set in a quartz tube. After sealing under a primary vacuum, the latter was heated (sweep rate = 1.5 °C/min) at 1100 °C for 24 h and finally quenched at room temperature. From these experimental conditions, a melt sample was obtained. In this batch, black shiny crystals, typically 100 × 100 × 80 μm^3 in size, were extracted and tested on a Kappa CCD (Bruker Nonius) four-circle diffractometer.

This study has revealed a P-type trigonal lattice for the major platelike crystals with the following cell parameters: $a \approx 5.65$ Å and $c \approx 18.8$ Å. To complete this preliminary structural work, we crushed a cluster of crystals in alcohol for studying by transmission electron microscopy (TEM). This work has been carried out with a JEOL 2010 Cx working at 200 kV and equipped with an Oxford analyzer. The electron diffraction (ED) patterns have confirmed the P trigonal cell (5.65 × 5.65 × 18.8 $Å^3$), without reflection conditions (Figure 1), while the analytical measurements by electron dispersion spectroscopy (EDS) yielded to a cationic composition "$Ba_6Ga_{2.3}Co_{11.4}$". We must emphasize that during this TEM analysis, other cobalt-rich crystallites have been identified. They also exhibited lattices related to hexagonal structures associated with significant shifts in cationic compositions and different periodicities along the c^* axis. Such observations suggest the existence of several layered oxides belonging to the same structural series.

Single-crystal X-ray diffraction was performed using Mo K_α radiations. Large Ω- and Φ-scans were used to control the crystalline quality and determine the unit-cell parameters. A single crystal of suitable size (80 × 80 × 80 μm^3) was selected. For room temperature measurements we defined a suitable data collection strategy by considering the cell parameters and the spot sizes. A scanning angle of 0.8° and a *Dx* (detector−sample distance) value of 34 mm were chosen; Φ- and Ω-scans were used. To collect a great number of weak reflections without saturation by reflections of strong intensity, we used two different exposure times (45 s/deg and 5 s/deg). The diffracted intensities were collected up to $\theta = 42°$. Three independent trigonal spaces were scanned.

Crystal Structure Determination

Plots of reciprocal lattice planes assembled from these series of experimental frames are sufficiently accurate to obtain an overall view of the reciprocal space. The diffraction pattern can be described within a P-type trigonal cell and the following parameters: $a = 5.652(2)$ Å, $b = 5.652(2)$ Å, $c = 18.828(8)$ Å, $\gamma = 120°$.

Because no condition limiting the possible reflections is observed, the possible space groups are $P3$, $P\bar{3}$, $P321$, $P3m1$, $P\bar{3}m1$, $P312$, $P31m$, and $P\bar{3}1m$. The EvalCCD software[11] was used to extract reflections from the collected frames and reflections were merged and rescaled as a function of the exposure time. The analysis of the diffracted intensities via the observation of the (hk0) reciprocal lattice planes or via a comparison of the internal reliability factor for the different Patterson symmetries ($R_{int} = 14.5\%$ for $\bar{3}$, 14.8% for $\bar{3}m1$ and 49% for $\bar{3}1m$) allows us to reject the $P312$, $P31m$, and $P\bar{3}1m$ space groups. Next, data were corrected from absorption using the crystal shape and Gaussian integration method; it follows an R_{int} value decreasing to 4.8 and 5% for $\bar{3}$ and $\bar{3}m1$, respectively.

A structural model considering the $P\bar{3}m1$ space group has been built with SIR2002[12] using direct methods. Next, 3 barium, 7 cobalt, and 5 oxygen independent atoms were located. This model was subsequently introduced in the refinement program Jana2000,[13] all the atomic positions were refined and finally anisotropic atomic displacement parameters were considered for all the atoms (the refinements led to the final agreement factors $R(obs) = 3.3\%$, $R_w(obs) = 3.2\%$). The chemical formula $Ba_6Ga_2Co_{11}O_{26}$ deduced from the refinements is in agreement with the cationic ratio determined by EDS analysis. Nevertheless, it has not been possible to evidence a Ga/Co ordering or discriminate the presence of gallium on a specific site from our X-ray diffraction data. Because we have to consider that cobalt and gallium species are ramdomely distributed on common sites, only the "Co" polyhedra are discussed in the crystal structure de-

(11) Duisenberg, A.; Kroon-Batenburg, L.; Shreurs, A. *J. Appl. Crystallogr.* **2003**, *36*, 220.
(12) Burla, M.; Camalli, M.; Carrozzini, B.; Cascarano, G. L.; Giacovazzo, C.; Polidori, G.; Spagna, R. *SIR2002*; Institute of Crystallography: Bari, Italy, 2002.
(13) Petricek, V.; Dusek, M. *Jana 2000, The Crystallographic Computing System*; Institute of Physics: Praha, Czech Republic, 2000.

Table 1. Positional and ADP Harmonic Parameters

Positional Parameters

atom	*x*	*y*	*z*	U_{eq} (Å^2)
Ba(1)	0	0	0.19115(2)	0.00831(8)
Ba(2)	0.3333	0.6667	0.32961(2)	0.00813(8)
Ba(3)	0.6667	0.3333	0.44466(2)	0.00846(8)
Co(1)	0.5	0	0	0.00452(17)
Co(2)	0	0	0	0.0071(2)
Co(3)	0.3333	0.6667	−0.12254(5)	0.00495(16)
Co(4)	0.3333	0.6667	0.15147(5)	0.00621(17)
Co(5)	0.3333	0.6667	−0.26712(5)	0.00666(17)
Co(6)	0	0	0.36934(5)	0.00523(17)
Co(7)	0	0	0.5	0.0053(2)
O(1)	0.3333	0.6667	0.0517(3)	0.0073(9)
O(2)	0.1797(3)	−0.1797(3)	−0.05734(15)	0.0063(6)
O(3)	0.5117(3)	0.0235(6)	0.18441(16)	0.0086(7)
O(4)	0.8373(3)	0.1627(3)	0.31307(16)	0.0089(7)
O(5)	0.8520(3)	−0.2960(6)	0.56392(16)	0.0080(7)

ADP Harmonic Parameters (Å^2)

	u_{11}	u_{22}	u_{33}	u_{12}	u_{13}	u_{23}
Ba(1)	0.00640(10)	0.00640(10)	0.01213(15)	0.00320(5)	0	0
Ba(2)	0.00710(10)	0.00710(10)	0.01019(15)	0.00355(5)	0	0
Ba(3)	0.00680(10)	0.00680(10)	0.01177(15)	0.00340(5)	0	0
Co(1)	0.00343(19)	0.0035(2)	0.0067(2)	0.00176(12)	−.00006(9)	−0.00011(2)
Co(2)	0.0058(3)	0.0058(3)	0.0095(5)	0.00292(14)	0	0
Co(3)	0.00453(19)	0.00453(19)	0.0058(3)	0.00226(10)	0	0
Co(4)	0.0058(2)	0.0058(2)	0.0070(3)	0.00291(10)	0	0
Co(5)	0.0062(2)	0.0062(2)	0.0076(3)	0.00310(10)	0	0
Co(6)	0.00446(19)	0.00446(19)	0.0068(3)	0.00223(10)	0	0
Co(7)	0.0047(3)	0.0047(3)	0.0064(4)	0.00237(14)	0	0
O(1)	0.0061(11)	0.0061(11)	0.0097(17)	0.0031(5)	0	0
O(2)	0.0052(7)	0.0052(7)	0.0078(9)	0.0022(8)	-0.0002(4)	0.0002(4)
O(3)	0.0083(8)	0.0058(10)	0.0107(11)	0.0029(5)	0.0002(4)	0.0004(8)
O(4)	0.0082(8)	0.0082(8)	0.0124(12)	0.0057(9)	-0.0012(4)	0.0012(4)
O(5)	0.0076(8)	0.0068(10)	0.0093(10)	0.0034(5)	0.0005(4)	0.0010(8)

Table 2. Interatomic Distances (Å)[a]

Ba(1)−O(2)^{i}	3.072(3)	Ba(2)−O(3)^{ix}	3.244(3)	Ba(3)−O(4)	2.988(3)
Ba(1)−O(2)^{ii}	3.072(3)	Ba(2)−O(3)^{vi}	3.244(3)	Ba(3)−O(4)^{x}	2.988(3)
Ba(1)−O(2)^{iii}	3.072(3)	Ba(2)−O(3)^{viii}	3.244(3)	Ba(3)−O(4)^{viii}	2.988(3)
Ba(1)−O(3)^{iv}	2.831(2)	Ba(2)−O(4)^{iv}	2.8434(12)	Ba(3)−O(5)^{ix}	2.887(3)
Ba(1)−O(3)	2.831(2)	Ba(2)−O(4)^{ix}	2.8434(12)	Ba(3)−O(5)^{xii}	2.836(2)
Ba(1)−O(3)^{v}	2.831(4)	Ba(2)−O(4)^{vi}	2.843(2)	Ba(3)−O(5)^{xv}	2.836(3)
Ba(1)−O(3)^{vi}	2.831(4)	Ba(2)−O(4)^{x}	2.843(2)	Ba(3)−O(5)^{v}	2.887(3)
Ba(1)−O(3)^{vii}	2.8312(19)	Ba(2)−O(4)^{viii}	2.843(2)	Ba(3)−O(5)^{xvi}	2.836(4)
Ba(1)−O(3)^{viii}	2.831(2)	Ba(2)−O(4)^{xi}	2.843(2)	Ba(3)−O(5)^{xiii}	2.836(4)
Ba(1)−O(4)^{iv}	2.794(3)	Ba(2)−O(5)^{xii}	2.704(3)	Ba(3)−O(5)^{xvii}	2.887(3)
Ba(1)−O(4)^{v}	2.794(3)	Ba(2)−O(5)^{xiii}	2.704(3)	Ba(3)−O(5)^{xviii}	2.836(2)
Ba(1)−O(4)^{viii}	2.794(3)	Ba(2)−O(5)^{xiv}	2.704(3)	Ba(3)−O(5)^{xix}	2.8365(19)
Co(1)-O(1)^{xx}	1.900(3)	Co(2)-O(2)	2.064(2)	Co(3)-O(2)^{ix}	1.942(2)
Co(1)-O(1)^{xxi}	1.900(3)	Co(2)-O(2)^{i}	2.064(2)	Co(3)-O(2)^{vi}	1.942(2)
Co(1)−O(2)	1.907(2)	Co(2)−O(2)^{vi}	2.064(2)	Co(3)−O(2)^{viii}	1.942(2)
Co(1)−O(2)^{xxii}	1.907(2)	Co(2)−O(2)^{ii}	2.064(2)	Co(3)−O(3)^{xxi}	1.912(3)
Co(1)−O(2)^{xxiii}	1.907(3)	Co(2)−O(2)^{vii}	2.064(2)	Co(3)−O(3)^{xxiv}	1.912(3)
Co(1)−O(2)^{iii}	1.907(3)	Co(2)−O(2)^{iii}	2.064(2)	Co(3)−O(3)^{iii}	1.912(3)
Co(4)−O(1)	1.878(5)	Co(5)−O(3)^{xxi}	2.174(3)	Co(6)−O(4)^{iv}	1.913(2)
Co(4)−O(3)^{ix}	1.853(3)	Co(5)−O(3)^{xxiv}	2.174(3)	Co(6)−O(4)^{v}	1.913(2)
Co(4)-O(3)^{vi}	1.853(3)	Co(5)-O(3)^{iii}	2.174(3)	Co(6)-O(4)^{viii}	1.913(2)
Co(4)−O(3)^{viii}	1.853(3)	Co(5)−O(4)^{xxi}	1.881(2)	Co(6)−O(5)^{xii}	1.918(3)
		Co(5)−O(4)^{xxiv}	1.881(2)	Co(6)−O(5)^{xxv}	1.918(3)
		Co(5)−O(4)^{iii}	1.881(2)	Co(6)−O(5)^{xviii}	1.918(3)
Co(7)−O(5)^{iv}	1.883(3)				
Co(7)−O(5)^{xii}	1.883(3)				
Co(7)−O(5)^{v}	1.883(3)				
Co(7)−O(5)^{xxv}	1.883(3)				
Co(7)−O(5)^{viii}	1.883(3)				
Co(7)−O(5)^{xviii}	1.883(3)				

[a] Symmetry codes: (i) $-x, -y, -z$; (ii) $y, -x+y, -z$; (iii) $x-y, x, -z$; (iv) $-1+x, y, z$; (v) $-y, -1+x-y, z$; (vi) $-y, x-y, z$; (vii) $-x+y, -x, z$; (viii) $1-x+y, 1-x, z$; (ix) $x, 1+y, z$; (x) $1-y, x-y, z$; (xi) $1-x+y, 2-x, z$; (xii) $1-x, -y, 1-z$; (xiii) $1+y, 2-x+y, 1-z$; (xiv) $-1+x-y, x, 1-z$; (xv) $2-x, -y, 1-z$; (xvi) $1+y, 1-x+y, 1-z$; (xvii) $2-x+y, 1-x, z$; (xviii) $-1+x-y, -1+x, 1-z$; (xix) $x-y, x, 1-z$; (xx) $x, -1+y, z$; (xxi) $1-x, 1-y, -z$; (xxii) $1-x, -y, -z$; (xxiii) $1-x+y, -x, z$; (xxiv) $y, 1-x+y, -z$; (xxv) $y, 1-x+y, 1-z$

scription part. Corresponding atomic positions and main interatomic distances are reported in Tables 1 and 2, respectively.

The same structural solution is obtained using the other space groups, *P*3, P$\bar{3}$, *P*321, or *P*3*m*1, without significant improvements of our model. Consequently, only the refine-

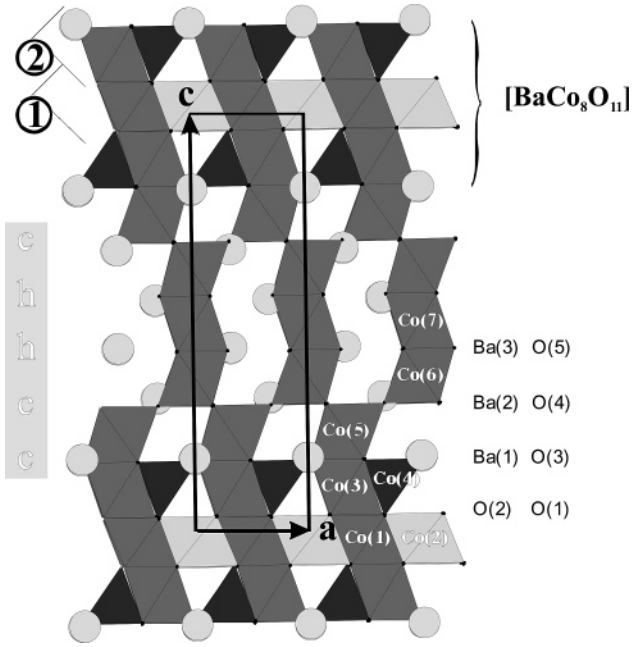

Figure 2. [010] projection of the $Ba_6Ga_2Co_{11}O_{26}$ phase. It can be divided in two parts: 5H-hexagonal perovskite block, labeled *chhcc*, and $BaCo_8O_{11}$ block built of two specific layers, namely 1 and 2. Tetrahedra and dark and light gray octahedra are associated with CoO_4 and CoO_6 environments. Ba atoms are represented by light gray disks.

ment results performed with the $P\bar{3}m1$ space group will be discussed in the following.

Crystal Structure Description and Discussion

Clearly, the structural analysis of $Ba_6(Ga,Co)_{13}O_{26}$ leads to a complex, cobalt-rich layered oxide. The projection of the structure along the *b* axis (Figure 2) combined with the cation−oxygen distances (Table 2) reveals the environment of the cations. Thus, the three barium sites are surrounded by 12 oxygen first neighbors (2.704 Å ≤ d_{Ba-O} ≤ 3.244 Å). The atoms located in the Co(1), Co(2), Co(3), Co(5), Co(6), and Co(7) sites are in CoO_6 octahedral environments, whereas the one in the Co(4) site is in a CoO_4 tetrahedral environment. Let us consider the Co_4O_8 slab labeled 1 in Figure 2; its projection along *c* is drawn in Figure 3a. The $Co(1)O_6$ octahedra are characterized by six short Co−O distances close to 1.90 Å, whereas the $Co(2)O_6$ octahedra exhibit six long Co−O distances (2.06 Å). The $Co(1)O_6$ share four edges with $Co(1)O_6$ octahedra and two with $Co(2)O_6$, whereas $Co(2)O_6$ share six edges with $Co(1)O_6$ octahedra. The adjacent $BaCo_2O_3$ slab, labeled 2 in Figure 2, is built from $Co(3)O_6$ octahedra and $Co(4)O_4$ tetrahedra linked by apex-forming windows over-hanged by Ba(1) atoms. The $Co(4)O_4$ and three $Co(1)O_6$ share one apex O(1), whereas $Co(3)O_6$ share each of its three O(2) apexes with two $Co(1)O_6$ and one $Co(2)O_6$. Cobalt atoms labeled Co(5) exhibit three long Co−O distances equal to 2.17 Å and three short distances of 1.88 Å; the resulting $Co(5)O_6$ octahedron shares one face with one $Co(3)O_6$ octahedron and three apexes with three $Co(6)O_6$ octahedra. The cobalt atoms labeled Co(6) and Co(7) exhibit a quite similar environment characterized by six short Co−O distances (close to 1.9 Å). The octahedra $Co(6)O_6$ and $Co(7)O_6$ are connected by faces.

The bond valence analysis of these different interatomic distances allows us to propose various oxidation states for cobalt species: Co(1) and Co(7) environments are compatible with Co^{4+}, whereas the Co(2) environment is consistent with Co^{2+}. The other cobalt sites can be associated with trivalent cobalt. Taking into account the ability of Ga^{3+} to adopt the tetrahedral coordination, we can guess that the Co(4) site is mainly occupied by Ga species. The four bonds observed (4 × 1.86 Å) are very similar to those observed (4 × 1.88 Å) in $BaGa_{12}O_{19}$ oxide related to the magnetoplumbite structure.[10]

From the projection shown in Figure 2, the stacking can be described as a regular intergrowth between a $BaCoO_3$-type hexagonal perovskite and an unusual layered $Ba(Ga,Co)_8O_{11}$ block sharing a BaO_3 layer with the other block.

Taking into account the stacking observed along the *c* axis in the perovskite block, the (*cchhc*) sequence related to 5H-perovskite can be proposed for the first part of this complex intergrowth.

The second block, namely $Ba(Ga,Co)_8O_{11}$, is more complex to describe. It can be analyzed as a pure Co-based Co_4O_8 slab made of edge-shared CoO_6 octahedra (Figure 3a) sandwiched between two mixed $Ba(Co,Ga)_2O_3$ slabs built from corner-shared GaO_4 tetrahedra and CoO_6 octahedra surrounding a Ba site (Figure 3b). Several structural analogies can be found in the literature to clarify this $Ba(Ga,Co)_8O_{11}$ block. Thus, the kamiokite $Fe_2Mo_3O_8$ mineral,[14] related to a nolanite structure,[15] reveals close structural relationships, because it can be analyzed as the alternating of a M_3O_4 layer made from three edge-shared MoO_6 octahedra (M), like that observed along the [111] direction of the spinel structure (Figure 4a), and a MTO_4 layer made from corner-shared FeO_4 tetrahedra (T) and FeO_6 octahedra (M) forming a cavity in which an extra oxygen atom sits (Figure 4b). So the $Ba(Ga,Co)_8O_{11}$ block is derived from the latter structure considering an extra Co site inside the M_3O_4 layer, forming Co_4O_4 (label 1 in Figure 2) similar to the $[111]^{RS}$ layer observed in the CoO oxide[17], and considering the replacement of the extra oxygen by a Ba species in the MTO_4 layer to form a $Ba(Co,Ga)_2O_3$ nolanite-type layer (label 2 in Figure 2). Considering a close-packed arrangement, the whole sequence observed in this block is $BaO_3-(Ga,Co)_2-O_4-Co_4-O_4-(Ga,Co)_2-BaO_3$.

A general description can also be proposed using M and T labels for octahedrally and tetrahedrally coordinated cations, respectively. Thus, the present stacking modes can be written $O_4-MT-O_4-M_3-O_4-MT-O_4$ for the TM_4O_8 nolanite-type structure, $O_4-M_4-O_4-M_4-O_4$ for the $[111]^{RS}$ CoO oxide, and $BaO_3-MT-O_4-M_4-O_4-MT-BaO_3$ for the $Ba(Ga,Co)_8O_{11}$ block. On the other hand, the structure of the $BaGa_2Co_6O_{11}$ block can be described from one Co_4O_8 slab, related to CdI_2-type slices (Figure 3a) and sandwiched by two $Ba(Co,Ga)_2O_3$ slabs exhibiting a nolanite type structure (Figure 3b) in which the close-packed BaO_3 layer is common with the hexagonal perovskite block.

(14) Hanson, A. W. *Acta Crystallogr.* **1958**, *11*, 703.
(15) Bertrand, D.; Kerner-Czeskleba, H. *J. Phys. (Paris)* **1975**, *36*, 379.

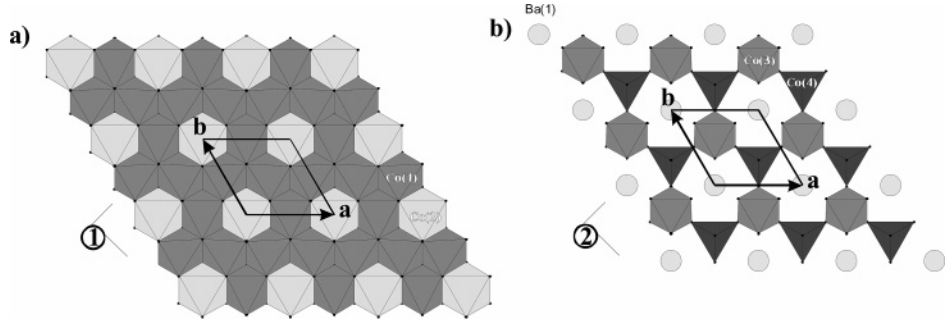

Figure 3. Projection along the [001] direction of (a) Co_4O_8 and (b) $Ba(Co,Ga)_2O_3$ slabs, labeled 1 and 2 in Figure 2, respectively, forming the $[Ba(Co,Ga)_8O_{11}]$ block.

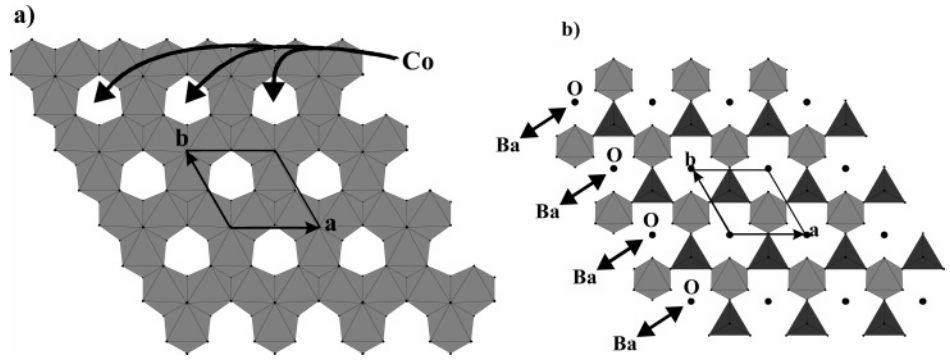

Figure 4. Projection along [001] direction of (a) M_3O_4 and (b) TMO_4 layers, Mo_3O_4 and Fe_2O_4, respectively, forming the kamiokite $Fe_2Mo_3O_8$ mineral.

Conclusions

The present structural study shows the existence of a new compound, $Ba_6(Ga,Co)_{13}O_{26}$. Its structural description results from an intergrowth model between an hexagonal perovskite and complex $[Ba(Ga,Co)_8O_{11}]$ blocks. It has been shown that this phase belongs to the series of compounds $[Ba(Ga,Co)_8O_{11}]$ $[BaCoO_3]_n$, where n is the number of the oxygen layers in the hexagonal perovskite block. In this framework, the $Ba_6(Ga,Co)_{13}O_{26}$ oxide represents the $n = 5$ term of this series. It must be noticed that this structural description differs from that reported for the $Ba_{n+1}Co_nO_{3n+3}(Co_8O_8)$ series,[8] especially at the level of the junction layer between the hexagonal perovskite block and the Co_4O_8 layers. In our description, the Co_4O_8 central layer, which is related to a CdI_2-type slice, is sandwiched between two $Ba(Co,Ga)_2O_3$ nolanite-type layers. By stacking this new $Ba(Ga,Co)_8O_{11}$ close-packed arrangement to different hexagonal perovskite polytypes, one can predict the existence of numerous members belonging to this series in agreement with the report of $Ba_2Co_9O_{14}$ ($n = 1$) and $Ba_3Co_{10}O_{17}$ ($n = 2$) oxides[8] and with our first TEM observations. The analysis of interatomic distances observed in edge-shared CoO_6 forming the Co_4O_8 layer suggests the existence of a Co^{2+}/Co^{4+} ordering in favor of a charge localization in the $[Ba(Ga,Co)_8O_{11}]$ block. The crystal growth of the different terms, with or without Ga^{3+} species, and the study of their physical properties are in progress. All these results are promising to observe interesting physical properties as a thermoelectric power or a multiferroic behavior as illustrated by the dielectric $Ba_8CoNb_6O_{24}$ hexagonal perovskite.[16]

Acknowledgment. The authors are grateful to H. Rousselière for technical support.

Supporting Information Available: Crystallographic information in CIF format. This material is available free of charge via the Internet at http://pubs.acs.org.

CM0702823

(16) Mallison, P. M.; Allix, M.; Claridge, J. B.; Ibberson, R. M.; Iddes, D. M.; Price, T.; Rosseinsky, M. J. *Angew. Chem., Int. Ed.* **2005**, *44*, 7733.